JACS
JOURNAL OF THE AMERICAN CHEMICAL SOCIETY
Communication
pubs.acs.org/JACS

Simplest *N*-Sulfonylamine $HNSO_2$

Guohai Deng,[†] Zhuang Wu,[†] Dingqing Li,[†] Roberto Linguerri,[§] Joseph S. Francisco,*[,‡] and Xiaoqing Zeng*[,†]

[†]College of Chemistry, Chemical Engineering and Materials Science, Soochow University, Suzhou 215123, China
[‡]Department of Chemistry, Purdue University, West Lafayette, Indiana 47907, United States
[§]Laboratorie de Modelisation et Simulation Multi Echelle, Universite Paris-Est, 77454 Marne La Vallee, France

Supporting Information

ABSTRACT: The simplest *N*-sulfonylamine $HNSO_2$ has been generated in the gas phase through flash vacuum pyrolysis of methoxysulfonyl azide $CH_3OS(O)_2N_3$. Its identification was accomplished by combining matrix-isolation IR spectroscopy and quantum chemical calculations. Both experimental and theoretical evidence suggest a stepwise decomposition of the azide via the methoxysulfonyl nitrene $CH_3OS(O)_2N$, observed in the 193 nm laser photolysis of the azide, with concerted fragmentation into CH_2O and $HNSO_2$. Upon the 193 nm laser irradiation, $HNSO_2$ isomerizes into the novel *N*-hydroxysulfinylamine HONSO.

Inorganic small molecules containing S, N, and O have attracted increasing interest due to the important roles in chemistry,[1] biology,[2] and atmosphere.[3] For instance, radicals SNO/NSO[4] and the corresponding anions SNO^-/NSO^-[5] have been regarded as candidate species in atmospheric and astrochemistry. Moreover, the acid molecules HSNO and HNSO have been the targets of extensive experimental and theoretical studies.[6] Particularly, the smallest *S*-nitrosothiol, HSNO, has been found to be generated during the physiological metabolism of H_2S and act as a key signaling molecule that can freely diffuse through membranes for protein *S*-nitrosation.[7]

Molecules solely consisting of $[NO_2S]$ are also known. Among the various isomers, OSNO was observed in cryogenic matrices during the photolysis of OCS and NO_2.[8] Recently, O_2SN was identified among the pyrolysis products of sulfonyl azide $CF_3S(O)_2N_3$.[9] The preparation of the cesium salt of the NSO_2^- anion has been claimed;[10a] however, subsequent comprehensive spectroscopy investigation of this material showed that it is comprised primarily of NSO^-.[10b] Nevertheless, the formation of NSO_2^- was found in the gas-phase ion/molecule reaction of NH_2^- and SO_2F_2, from which the acidity of $HNSO_2$ (330 ± 5 kcal mol^{-1}) at 333 K was estimated.[10c]

As for the acid, nine isomers including $HNSO_2$, HONSO, HOSNO, HOS(O)N, $HSNO_2$, HSONO, HON(O)S, HOOSN, and HOONS have been computationally explored.[11a] The planar $HNSO_2$, a close analogue of SO_3 (Scheme 1), is the global minimum on the potential energy surface. Importantly, the CCSD(T) calculated S−N bond dissociation energy in $HNSO_2$ (51.4 kcal mol^{-1}) is much higher than that in the atmospherically relevant radical H_2NSO_2 (17.6 kcal mol^{-1}).[11b]

Scheme 1. Lewis Structures of SO_3 and $HNSO_2$

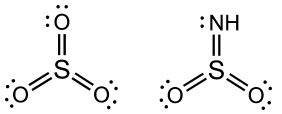

The second stable isomer is the open-chain HONSO (10.6 kcal mol^{-1}), which can be formally regarded as the hydroxyl compound of the pseudohalogen group NSO (Scheme 2). Notably, the much higher-energy thionitrate, $HSNO_2$, has been identified as an intermediate in the oxidation of H_2S under physiological conditions.[12]

Scheme 2. Calculated Relative Energies (kcal mol^{-1}) of $HNSO_2$ and HONSO at the CCSD(T)/6-311++G(2df, 2p) Level

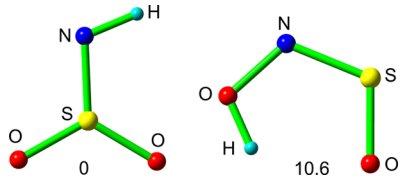

$HNSO_2$, the simplest *N*-sulfonylamine, remains experimentally unknown, although its existence was first proposed in the reaction of SO_3 with NH_3 by Goehring et al. in the 1950s.[13] Its intermediacy was inferred in the alkaline hydrolysis of the medicinally important aryl sulfamates.[14] According to the recent theoretical calculations,[14a] $HNSO_2$ should be an isolable species with markedly greater stability than SO_3 by 4.5 kcal mol^{-1}. It should be noted that the trimer of the acid, cyclotrisulfimide $(HNSO_2)_3$, has been prepared from hydrolysis of persilylated sulfanuric acid with HCl.[15] Herein, we report the generation, characterization, and photochemistry of $HNSO_2$, as well as the mechanism for its formation from $CH_3OS(O)_2N_3$ by combining quantum chemical calculations.

Inspired by the decomposition of $CH_3OC(O)N_3$ into CH_2O, HNCO, and N_2,[16] our synthetic approach to $HNSO_2$ utilizes methoxysulfonyl azide as the precursor. Specifically, a gas

Received: August 1, 2016
Published: August 30, 2016

DOI: 10.1021/jacs.6b07966
J. Am. Chem. Soc. 2016, 138, 11509−11512

mixture of $CH_3OS(O)_2N_3$ in Ne, Ar, or N_2 dilution (ca. 1:1000) was passed through a heated Al_2O_3 furnace (ca. 1000 K), the decomposition products were immediately condensed onto the cold surface of Rh-plated copper block (2.8 K) for IR spectroscopy analysis.[4a]

The typical IR spectrum of the pyrolysis products in Ne matrix is shown in Figure 1 (upper trace). Only traces of the azide (a) were left undecomposed. As a result, CH_2O (d),[16] SO_2 (e),[9] N_2 (IR inactive), and a new species exhibiting strong IR bands (c) at 3354.1, 1391.7, 1291.2, 1049.0, 970.3, and 657.9 cm^{-1} were obtained. No IR bands of counterpart CH_3NO were identified probably due to low IR intensities. In contrast, the title compound $HNSO_2$ was attributed to be the carrier of the aforementioned six IR bands by comparing with the predicted IR spectrum (Table 1).

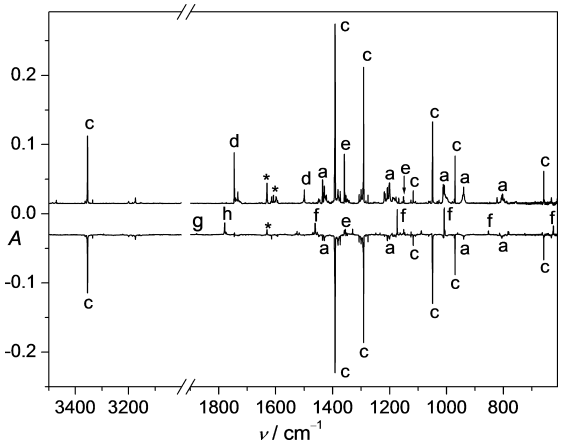

Figure 1. Upper trace, Ne-matrix IR spectrum of the flash vacuum pyrolysis products of $CH_3OS(O)_2N_3$; lower trace, matrix IR difference spectrum showing the changes of the matrix upon a 193 nm laser photolysis. IR bands of $CH_3OS(O)_2N_3$ (a), $HNSO_2$ (c), H_2CO (d), SO_2 (e), HONSO (f), NO (g), HSONO (h), and H_2O (*) are marked.

The band at 3354.1 cm^{-1} for $HNSO_2$ is assigned to the N—H stretch (ν_1) due to the characteristic ^{15}N (7.2 cm^{-1}) and H/D (869.2 cm^{-1}) isotope shifts (Figures S1–S3). The strongest band at 1391.7 cm^{-1} belongs to the OSO asymmetric stretch (ν_2), the large band intensity enables a clear identification of the associated IR band at 1373.4 cm^{-1} for the naturally abundant ^{34}S. The frequency is higher than the OSO asymmetric stretch in O_2SN (1358.6 cm^{-1})[9] but very close to that in the isoelectronic SO_3 (1385.2 cm^{-1}).[17] The OSO symmetric stretch in $HNSO_2$ is strongly coupled with the S═N stretch, leading to an asymmetric OSN stretch (ν_3) with an observed frequency of 1291.2 cm^{-1}. Instead, the pure S═N stretch appears at 970.3 cm^{-1} with a large ^{15}N isotope shift ($\Delta\nu(^{14/15}N)$) of 17.2 cm^{-1}, the band position is very close to that in the radical O_2SN (966.9 cm^{-1}, $\Delta\nu(^{14/15}N)$ = 17.8 cm^{-1}).[9]

Additionally, another two IR bands at 1049.0 and 657.9 cm^{-1} for the in-plane (i.p.) and out-of-plane (o.o.p.) deformation of the N—H moiety were also observed, respectively. The former shows a large shift of 58.3 cm^{-1} upon deuteration, whereas, the latter shifts out of the available spectral range in this study (5000–600 cm^{-1}). With the aid of ^{15}N labeling experiment, several weak combination and overtone bands at 2676.3 ($\nu_2 + \nu_3$), 2433.6 ($\nu_2 + \nu_4$), 2356.3 ($\nu_2 + \nu_5$), 2253.4 ($\nu_3 + \nu_5$), 1930.4 ($2\,\nu_5$), and 1117.1 cm^{-1} ($\nu_8 + \nu_9$) were also found for $HNSO_2$ (Tables S1 and S2).

The production of $HNSO_2$ through the flash vacuum pyrolysis of $CH_3OS(O)_2N_3$ is completely reproducible by using Ar or N_2 as the carrier gas (Figures S3 and S4). The band positions observed for $HNSO_2$ in different matrices (Table 1) are slightly shifted due to weak interactions with the neighboring molecules. Based on the observed and calculated band intensities for the common OSO asymmetric stretching vibration modes in $CH_3OS(O)_2N_3$, $HNSO_2$, and SO_2, the yields of $HNSO_2$ and SO_2 were estimated to be about 75% and 7%, respectively. Such high yield of $HNSO_2$ facilitates a further study on its photochemistry in cryogenic matrices.

According to the predicted UV/vis spectrum (Table S3), the lowest-energy transition for $HNSO_2$ locates at 222 nm with oscillator strength of 0.0013. Therefore, an ArF excimer laser (193 nm, 7 mJ, 3 Hz) was utilized for the photolysis of the matrix containing the pyrolysis products of $CH_3OS(O)_2N_3$. The resulting IR difference spectrum reflecting the changes of the matrix upon irradiation is depicted in Figure 1 (lower trace). Traces of SO_2 (e) and several unknown species exhibiting weak IR signals were generated. The set of bands (marked by f in Figure 1) at 1461.5, 1173.0, 1007.7, 852.6, and 624.5 cm^{-1} demonstrate same photobehavior and show good agreement with the predicted IR spectrum of the second lowest-energy isomer HONSO (Table S4).

Table 1. Observed and Calculated IR Frequencies and Isotopic Shifts (cm^{-1}) for $HNSO_2$

calculated			observed in matrices[d]			$\Delta\nu(^{14/15}N)$[e]		$\Delta\nu(^{32/34}S)$[e]		$\Delta\nu$(H/D)[e]		
CASSCF[a]	B3LYP[b]	CCSD(T)[c]	Ne	Ar	N_2	calcd	exptl	calcd	exptl	calcd	exptl	assignment[f]
3758	3510 (66)	3514	3354.1 (32)	3328.9	3329.4	7.8	7.2	0	<0.5	942.8	869.2	ν_1, ν(NH)
1445	1401 (194)	1403	1391.7 (100)	1384.5	1387.4	0.5	0.5	18.8	18.3	6.1	5.0	ν_2, ν_{asym}(OSO)
1365	1304 (158)	1297	1291.2 (59)	1285.3	1300.5	8.2	7.7	16.1	15.7	13.7	11.4	ν_3, ν_{asym}(NSO)
1138	1075 (82)	1089	1049.0 (29)	1045.6	1058.8	3.6	4.1	0.1	<0.5	69.5	58.3	ν_4, $\delta_{i.p.}$(NH)
1044	986 (40)	979	970.3 (15)	967.1	986.6	18.1	17.2	0.6	<0.5	166.3	160.5	ν_5, ν(SN)
714	669 (71)	673	657.9 (9)	655.2	672.6	1.6	1.4	0.1	<0.5	151.4		ν_8, $\delta_{o.o.p.}$(NH)
549	519 (21)	517				2.1		2.5		23.0		ν_6, δ(SO_2)
504	466 (34)	461				4.9		2.0		12.3		ν_7, δ(OSN)
501	453 (28)	442				2.1		7.9		22.2		ν_9, $\delta_{o.o.p.}$(NSO_2)

[a]Calculated IR frequencies at the CASSCF/aug-cc-pV(T+d)Z level. [b]Calculated IR frequencies and intensities (km mol^{-1}) at the B3LYP/6-311++G(3df,3pd) level. [c]Calculated IR frequencies at the CCSD(T)/6-311++G(2df,2p) level. [d]Observed IR band positions in Ne, Ar, and N_2 matrices, the integrated relative intensities for the bands observed in Ne matrix are given in parentheses. [e]The $^{14/15}N$, $^{32/34}S$, H/D isotopic shifts. [f]Assignment based on the calculated vibrational displacement vectors.

DOI: 10.1021/jacs.6b07966
J. Am. Chem. Soc. 2016, 138, 11509–11512

The two bands at 1007.7 and 852.6 cm^{-1} for HONSO bear large ^{15}N isotope shifts of 16.7 and 17.0 cm^{-1}, corresponding mainly to the O—N and N═S stretches, respectively. The band at 1173.0 cm^{-1} with a shift of 10.2 cm^{-1} for the naturally abundant ^{34}S belongs to the asymmetric NSO stretch, the frequency is lower than that in the Ne-matrix isolated NSO radical (1199.3 cm^{-1}, $\Delta\nu(^{14/15}N)$ = 5.6 cm^{-1}, $\Delta\nu(^{34/32}S)$ = 14.2 cm^{-1}).[4a] The two O−H deformation modes occur at 1461.5 ($\delta_{i.p.}$(OH)) and 624.5 cm^{-1} ($\delta_{o.o.p.}$(OH)), and a large H/D isotope shift of 220.3 cm^{-1} was observed for the former (Table S4). The O—H stretching vibration in HONSO predicted at 3473 cm^{-1} could not be identified.

In addition to HONSO and SO_2, traces of NO (1877.5 cm^{-1}, $\Delta\nu(^{14/15}N)$ = 33.1 cm^{-1})[18] and another NO-containing species with characteristic N═O stretching vibration at 1779.3 cm^{-1} ($\Delta\nu(^{14/15}N)$ = 30.8 cm^{-1}) were also produced. This band can be tentatively assigned to the open-chain HSONO, for which a very strong IR band at 1849 cm^{-1} with ^{15}N isotope shift of 33.0 cm^{-1} was predicted (Table S1). As can be seen in Figure 1 (lower trace), there are several even weaker IR bands remain unassigned, implying the complex photochemistry of $HNSO_2$.

To capture the intermediate and probe the underlying mechanism for the decomposition of $CH_3OS(O)_2N_3$, a Ne matrix containing the azide was subjected to the 193 nm laser irradiation, the IR difference spectrum is given in Figure 2

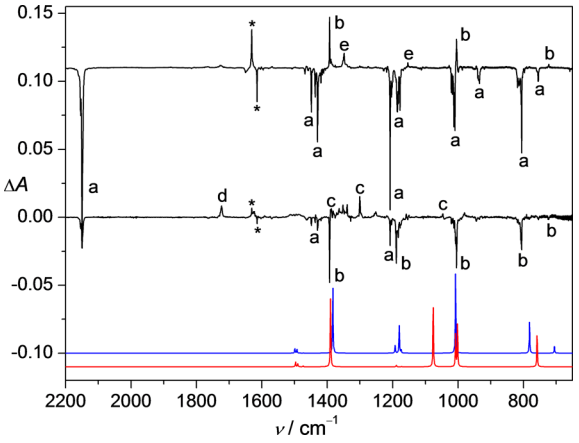

Figure 2. Upper trace, Ne-matrix IR difference spectrum showing the changes of the matrix-isolated $CH_3OS(O)_2N_3$ upon an 193 nm laser photolysis; middle trace, matrix IR difference spectrum showing the changes upon subsequent 266 nm photolysis; lower trace, calculated IR spectra of $CH_3OS(O)_2N$ in the singlet (red) and triplet (blue) states at the B3LYP/6-311++G(3df,3pd) level. IR bands of $CH_3OS(O)_2N_3$ (a), $CH_3OS(O)_2N$ (b), $HNSO_2$ (c), H_2CO (d), SO_2 (e), and H_2O (*) are marked.

(upper trace) and compared with the predicted spectra for the most likely candidate sulfonyl nitrene $CH_3OS(O)_2N$ in both singlet and triplet states (Figure 2, lower trace). Similar to the photochemistry of $CH_3S(O)_2N_3$,[19] the nitrene $CH_3OS(O)_2N$ in the triplet state (b) and traces of SO_2 (e) were identified as the products. The observed IR bands at 1392.2, 1188.7, 1005.3, 805.6, and 723.7 cm^{-1} coincide with the calculated frequencies of 1383, 1180, 1007, 781, and 705 cm^{-1} for triplet $CH_3OS(O)_2N$ (Table S5). Moreover, all these bands show no distinguishable shift upon ^{15}N labeling except for the last one, which exhibits a well-resolved shift of 10.3 cm^{-1} (Figure S5) for the S−N stretching vibration ($\Delta\nu_{calcd}(^{14/15}N)$ = 10.9 cm^{-1}). The observation of the triplet state in the cryogenic matrix is fully consistent with the predicted preference of the triplet over the singlet state by 10.9 kcal mol^{-1} at the CBS-QB3 level.

Upon subsequent UV light irradiation (266 nm), the IR bands of the nitrene vanished completely with the simultaneous formation of $HNSO_2$ (c) and H_2CO (d) (Figure 2, middle trace). This is in contrast to the Curtius-type rearrangement of $CH_3S(O)_2N$.[19] Instead, the photochemistry of $CH_3OS(O)_2N$ resembles the decomposition of $CH_3OC(O)N_3$ into H_2CO, HNCO, and N_2, in which the putative nitrene $CH_3OC(O)N$ was assumed to undergo 1,4-hydrogen shift from CH_3 to the electron deficient nitrogen atom with concerted fragmentation of the C−O bond.[16]

To unravel the mechanism, the potential energy surface for the decomposition of $CH_3OS(O)_2N_3$ were calculated and the results are summarized in Figure 3. Like most covalent azides,

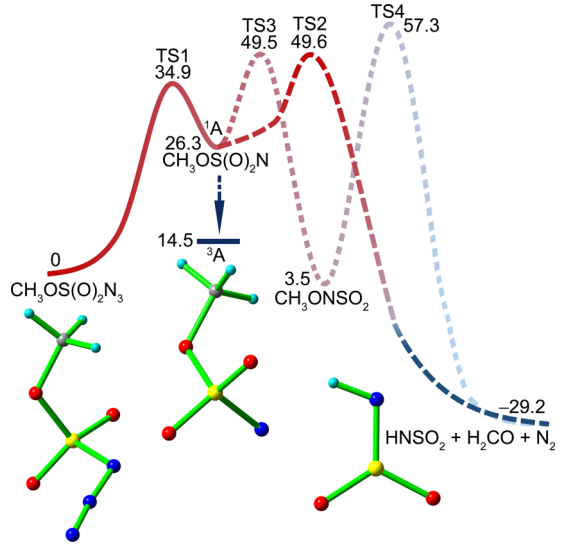

Figure 3. Potential energy curve (kcal mol^{-1}) for the decomposition of $CH_3OS(O)_2N_3$ calculated at the CCSD(T)/6-311++G(2df,2p)//UMP2/6-311++G(2df,2p) level of theory.

the decomposition of $CH_3OS(O)_2N_3$ into $CH_3OS(O)_2N$ and N_2 needs to surmount a moderate activation barrier of 34.9 kcal mol^{-1} at the CCSD(T)/6-311++G(2df,2p)//UMP2/6-311++G(2df,2p) level.

The initially generated singlet nitrene $CH_3OS(O)_2N$ may either relax to the triplet ground state or undergo two competing reactions with almost equal activation barriers. One is the Curtius-type rearrangement into CH_3ONSO_2 via the transition state TS3 with a barrier of 23.2 kcal mol^{-1}. However, CH_3ONSO_2 should be a kinetically stable species due to a formidable dissociation barrier (TS4, 53.8 kcal mol^{-1}) into $HNSO_2$ and H_2CO. The optional route is the 1,4-hydrogen shift from CH_3 to the nitrene center with concerted fragmentation of the C−O bond into $HNSO_2$ and H_2CO via TS2 with a barrier of 23.3 kcal mol^{-1} (Figure S6). Apparently, the absence of CH_3ONSO_2 among the pyrolysis products strongly supports a concerted decomposition mechanism for the initially singlet nitrene $CH_3OS(O)_2N$.

In conclusion, the long-sought SO_3 analogous molecule $HNSO_2$, has been prepared and characterized for the first time by combining matrix-isolation IR spectroscopy and quantum chemical calculations. A stepwise mechanism for the decomposition of the azide into $HNSO_2$, H_2CO, and N_2 was firmly

DOI: 10.1021/jacs.6b07966
J. Am. Chem. Soc. 2016, 138, 11509−11512

established by both the direct observation of the sulfonyl nitrene intermediate $CH_3OS(O)_2N$ and the computed potential energy surface. In addition, the photoinduced isomerization from $HNSO_2$ into the novel *N*-hydroxysulfinylamine HONSO was also observed. The facile production of $HNSO_2$ may stimulate further studies on the structure and reactivity of this fundamentally important species, and may also provide an access to the anion NSO_2^- through the reaction of the acid with strong base bearing bulky organic cation like tetrabutylammonium hydroxide.

■ ASSOCIATED CONTENT

Supporting Information

The Supporting Information is available free of charge on the ACS Publications website at DOI: 10.1021/jacs.6b07966.

Experimental details, calculation methods, matrix IR spectra, calculated IR spectra, and calculated atomic coordinates (PDF).

■ AUTHOR INFORMATION

Corresponding Authors

*X.Z. xqzeng@suda.edu.cn

*J.S.F. francisc@purdue.edu

Notes

The authors declare no competing financial interest.

■ ACKNOWLEDGMENTS

This work was supported by the National Natural Science Foundation of China (21372173, 21422304), the Priority Academic Program Development of Jiangsu Higher Education Institutions (PAPD).

■ REFERENCES

(1) (a) Chivers, T.; Laitinen, R. S. In *Handbook of Chalcogen Chemistry: New Perspectives in Sulfur, Selenium and Tellurium*, 2nd ed.; Vol. *1*; Devillanova, F. A.; du Mont, W. W., Eds.; RSC: Cambridge, 2013; pp 191−237. (b) Chivers, T. In *A Guide to Chalcogen-Nitrogen Chemistry*; World Scientific: London, 2005. (c) Longobardi, L.E.; Wolter, V.; Stephan, D. W. *Angew. Chem., Int. Ed.* **2015**, *54*, 809−812. (d) He, G.; Shynkaruk, O.; Lui, M. W.; Rivard, E. *Chem. Rev.* **2014**, *114*, 7815−7880.

(2) For very recent examples, see: (a) Basudhar, D.; Ridnour, L. A.; Cheng, R.; Kesarwala, A. H.; Heinecke, J.; Wink, D. A. *Coord. Chem. Rev.* **2016**, *306*, 708−723. (b) Cortese-Krott, M. M.; Butler, A. R.; Woollins, J. D.; Feelisch, M. *Dalton Trans.* **2016**, *45*, 5908−5919.

(3) For examples, see: (a) Mackenzie, R. B.; Dewberry, C. T.; Leopold, K. R. *Science* **2015**, *349*, 58−61. (b) Barnes, I.; Hjorth, J.; Mihalopoulos, N. *Chem. Rev.* **2006**, *106*, 940−975.

(4) (a) Wu, Z.; Li, D. Q.; Li, H. M.; Zhu, B. F.; Sun, H. L.; Francisco, J. S.; Zeng, X. Q. *Angew. Chem., Int. Ed.* **2016**, *55*, 1507−1510. (b) Fortenberry, R.; Francisco, J. S. *J. Chem. Phys.* **2015**, *143*, 084308-1−084308-7. (c) Yazidi, O.; Houria, A. B.; Francisco, J. S.; Hochlaf, M. *J. Chem. Phys.* **2013**, *138*, 104318-1−104318-12.

(5) Fortenberry, R. C.; Francisco, J. S. *J. Chem. Phys.* **2015**, *143*, 184301-1−184301-8.

(6) For examples, see: (a) Labbow, R.; Michalik, D.; Rei*β*, F.; Schulz, A.; Villinger, A. *Angew. Chem., Int. Ed.* **2016**, *55*, 7680−7684. (b) Hochlaf, M.; Linguerri, R.; Francisco, J. S. *J. Chem. Phys.* **2013**, *139*, 234304-1−234304-8.

(7) (a) Filipovic, M. R.; Miljkovic, J. L.; Nauser, T.; Royzen, M.; Klos, K.; Shubina, T.; Koppenol, W. H.; Lippard, S. J.; Ivanović-Burmazović, I. *J. Am. Chem. Soc.* **2012**, *134*, 12016−12027. (b) Miljkovic, J. L.; Kenkel, I.; Ivanović-Burmazović, I.; Filipovic, M. R. *Angew. Chem., Int. Ed.* **2013**, *52*, 12061−12064.

(8) Bahou, M.; Lee, Y.-P. *J. Chem. Phys.* **2001**, *115*, 10694−10700.

(9) Zeng, X. Q.; Beckers, H.; Willner, H. *Angew. Chem., Int. Ed.* **2013**, *52*, 7981−7984.

(10) (a) Roesky, H. W.; Schmieder, W.; Isenberg, W.; Böhler, D.; Sheldrick, G. M. *Angew. Chem., Int. Ed. Engl.* **1982**, *21*, 153. (b) Chivers, T.; Schmidt, K. J.; McIntyre, D. D.; Vogel, H. J. *Can. J. Chem.* **1989**, *67*, 1788−1794. (c) Morgon, N. H.; Linnert, H. V.; Riveros, J. M. *J. Phys. Chem.* **1995**, *99*, 11667−11672.

(11) (a) Méndez, M.; Francisco, J. S.; Dixon, D. A. *Chem. - Eur. J.* **2014**, *20*, 10231−10235. (b) Gao, Y.; Glarborg, P.; Marshall, P. *Z. Phys. Chem.* **2015**, *229*, 1649−1661.

(12) (a) Cuevasanta, E.; Zeida, A.; Carballal, S.; Wedmann, R.; Morzan, U.; Trujillo, M.; Radi, R.; Estrin, D.; Filipovic, M. R.; Alvarez, B. *Free Radical Biol. Med.* **2015**, *80*, 93−100. (b) Wedmann, R.; Zahl, A.; Shubina, T. E.; Dürr, M.; Heinemann, F. W.; Bugenhagen, B. E. C.; Burger, P.; Ivanović-Burmazović, I.; Filipovic, M. R. *Inorg. Chem.* **2015**, *54*, 9367−9380.

(13) Appel, R.; Goehring, M. *Angew. Chem.* **1952**, *64*, 616−617.

(14) (a) Williams, S. J.; Denehy, E.; Krenske, E. H. *J. Org. Chem.* **2014**, *79*, 1995−2005. (b) Spillane, W. J.; Thea, S.; Cevasco, G.; Hynes, M. J.; McCaw, C. J. A.; Maguire, N. P. *Org. Biomol. Chem.* **2011**, *9*, 523−530. (c) Winum, J.-Y.; Scozzafava, A.; Montero, J.-L.; Supuran, C. T. *Med. Res. Rev.* **2005**, *25*, 186−228.

(15) (a) Faleschini, G.; Nachbaur, E.; Belaj, F. *Phosphorus, Sulfur Silicon Relat. Elem.* **1992**, *65*, 147−150. (b) Appel, R.; Berger, G. *Z. Anorg. Allg. Chem.* **1964**, *327*, 114−123.

(16) Dyke, J. M.; Levita, G.; Morris, A.; Ogden, J. S.; Dias, A. A.; Algarra, M.; Santos, J. P.; Costa, M. L.; Rodrigues, P.; Andrade, M. M.; Barros, M. T. *Chem. - Eur. J.* **2005**, *11*, 1665−1676.

(17) Zhu, B. F.; Zeng, X. Q.; Beckers, H.; Francisco, J. S.; Willner, H. *Angew. Chem., Int. Ed.* **2015**, *54*, 11404−11408.

(18) Beckers, H.; Zeng, X. Q.; Willner, H. *Chem. - Eur. J.* **2010**, *16*, 1506−1520.

(19) Deng, G. H.; Li, D. Q.; Wu, Z.; Li, H. M.; Bernhardt, E.; Zeng, X. Q. *J. Phys. Chem. A* **2016**, *120*, 5590−5597 and references therein..

DOI: 10.1021/jacs.6b07966
J. Am. Chem. Soc. 2016, 138, 11509−11512